CIVIL ENGINEERING JOURNAL

Article no. 22

THE CIVIL ENGINEERING JOURNAL 2-2022

EXPERIMENTAL STUDY ON THE VERTICAL SELF-WEIGHT STRESS DISTRIBUTION LAW OF SLOPE WITH GRANULAR MATERIALS UNDER DIFFERENT CONDITIONS

Huijian Zhang, Gongning Liu, Weixiong Liu and Longgang Miao

Southwest Jiaotong University, Key laboratory of Transportation Tunnel Engineering. Ministry of Education, Chengdu, No. 111, North Section, Second Ring Road, Jinniu District, 610031, China; huijianz@163.com, 2995484603@qq.com, 695600270@qq.com, 695174032@qq.com

ABSTRACT

Topography is one of the important factors affecting the distribution of the self-weight stress field. However, granular materials are different from general continuum materials (such as fluids and solids). Only adopting the continuum theory research still has certain limitations, while the use of experimental methods can better reflect the actual stress state of the granular materials. Therefore, in order to further obtain the vertical self-weight stress distribution of single slope with granular materials, the indoor experimental study of quartz sand based on the point source method is carried out in this paper. The research results indicate that: The measured value of the vertical stress on the bottom surface of the quartz sand slope is generally smaller than the γh (Gravity × Buried depth) value of the corresponding point, and the closer the measuring point is to the slope top, the greater the difference between the test value and γh. Besides, the influence of slope heights and slope ratios on the vertical self-weight stress about slope with granular material is also analyzed. Stress depressions appear in some test conditions, that is, the measured stress peak on the bottom of the slope does not appear at the measuring point closest to the slope top. Whether there is a stress depression and the scope of the depression is mainly related to the slope height, while the slope ratio has little effect on it.

KEY WORDS

Granular material, Self-weight stress, Slope topography, Slope height, Slope ratio, Distribution law

INTRODUCTION

The self-weight stress field is the main initial stress field of most tunnel projects and slope projects, and its stress distribution law is very important to the stability analysis of related projects. The vertical self-weight stress is calculated through multiplying the buried depth by the gravity (γh) based on the premise that the ground is horizontal and the rock mass is a semi-infinite elastic body [1, 2]. In fact, there are many factors affecting the self-weight stress field. Xie et al. [3] studied the self-weight stress of the foundation considering sedimentation, and the results showed that the self-weight stress changed nonlinearly with the depth. Liu and Li [4] regarded the parallel layered rock mass as an equivalent transversely isotropic body, deduced the theoretical solution of the in-situ stress of the rock mass under its own weight, then analyzed the influence of the rock inclination angle and the elastic parameters about the rock mass on the horizontal principal stress. Liang [5] proposed the distribution characteristics of the ground stress about the deep-cut valley based on the research results of the rock mass stress in the Jinping Hydropower Project pivot area. Savage [6-7]

studied the in-situ stress field near the vertical cliff under the action of its own weight and put forward a theoretical solution suitable for the design of rock slope. In addition, the in-situ stress field of the finite elastic slope under self-weight load was also studied, the theoretical solution of the in-situ stress under the terrain was obtained and it can be used for the limited slope design with four kinds of slope angles. Yu et al [8] conducted numerical analysis on the ground self-weight stress field with the slope angles of 30°, 45° and 60°, respectively. The results showed that the difference between the slope vertical stress calculated by the direct buried depth and actual value of the slope was large under the self-weight condition. Qi and Wu [9] studied the stress field of the valley based on numerical simulation and in-situ stress measured data, and found that for a homogeneous elastic slope without unloading zone, the stress distribution from the slope surface to the inside slope can be divided into stress reduction area and stable stress area. While for the slope with unloading area, the stress distribution from the slope surface to the slope body can be divided into stress reduction area, stress rising area and stress stable area. Zhao et al [10] conducted statistical analysis on the distribution law of the in-situ stress field of China. For the stress field of the canyon slope, foreign scholars have also conducted a lot of theoretical and practical research [11-14]. In the literature [15], the self-weight stress was calculated according to the continuum mechanics assumption (finite element numerical simulation) of non-horizontal ground conditions. It was found that the vertical stress along the slope top line was smaller than the calculated value of “depth multiplied by severity”, especially when the slope was steep, the peak of the vertical stress was not even on the vertical line of the mountain top with the deepest buried depth, instead, the peak stress appeared at the two sides of the deepest buried depth section.

About the mechanical properties of granular materials, there have been certain studies at home and abroad. Vernay et al. [16] analyzed the unstable behavior of sand with different saturations under cyclic triaxial tests, and analyzed the influence of saturation on triggering these instabilities. It was found that even if the soil is not fully saturated initially, it can be liquefied. Wu et al. [17] used the discrete element method to study the mechanical properties of granular materials under various stress ratios and density conditions, and the respective ultimate states of different conditions were analyzed. Chen et al. [18] conducted three saturated cycle triaxial tests on granular material with high fines content, and further obtained its stable elastic modulus. It was found that with the increase of cyclic deviator stress, the elastic modulus of the granular material with high fine particle content first decreased and then gradually increased, and an improved non-monotonic relationship model for predicting the elastic modulus and the stress state was proposed. Based on discrete element software, the numerical model of the slope is established to analyze the stability and failure process of the slope [19-22], and the stability factors of the granular slope are also analyzed through experiments [23, 24].

Breaking through the continuum medium assumptions, it was found that there were some peculiar behaviors in the mechanical analysis based on the discrete particulate matter system. The famous granary effect [25] pointed out that when the height of grain accumulation was about twice the bottom diameter, the pressure on the bottom of the granary did not increase with the increase of grain. This was inconsistent with the conclusion that any buried depth pressure or vertical compressive stress was equal to the material weight multiplied by the buried depth in the traditional self-weight stress field. The German engineer Janssen explained that it was the silo wall supports part of the grain weight. Furthermore, removing the “silo” of the granary, in daily life, it was generally believed that when plenty of particles were naturally dumped on a level ground, the central pressure acting on the ground was the greatest. But this reality was not like this case, there was a stress value around the center, which was smaller than both sides and was the minimum value, and this phenomenon was called as stress depression [25]. The further research shows that the center of the sand heap may show a completely different stress distribution due to the different methods of forming the sand heap, the stress result of the falling rain method and the point source method was not the same [26]. Through the indoor falling rain method and PFC2D simulation software, Yao et al [27] analyzed the influence of particle size and friction coefficient on the stress characteristics of sand heap structure.

Granular materials have a wide range of applications in practice (such as embankment filling, grain piles, cofferdams, etc.), but the experimental research on the distribution of its vertical self-weight stress is still rarely involved. Besides, the mechanical properties of different soils are not the same, especially for slope with granular materials, there are still few studies. Therefore, on the basis of the above research, the further experimental research on the vertical self-weight stress distribution characteristics of the bottom surface of the quartz sand slope formed by the point source method is conducted in this paper, focusing on exploring the influence of slope height and slope ratio on the vertical self-weight stress about slope with granular material; further quantify the location and magnitude of the stress peak (the range of the stress depression), aiming to provide some theoretical support for the engineering design and construction of similar slope terrain.

INDOOR MODEL TEST DESIGN

Overall test scheme

In order to minimize the friction between the sand particles and the test box, glass test box is used in this test. As shown in Figure 1, the 2-4 mesh quartz sand is piled up by the point source method to form a unilateral slope in a glass box with the size of 1.5 m × 0.5 m × 0.55 m (length × width × height). A 10 cm thick cushion of the same material is set on the bottom of the slope in advance. To study the vertical stress distribution characteristics of sand slope under different conditions (various slope heights and slope ratios), vertical stress is obtained through several test sensors with the same size that are placed continuously on the cushion surface, the number of these test points is related to the horizontal length of the slope, ranging from 3 points to 8 points.

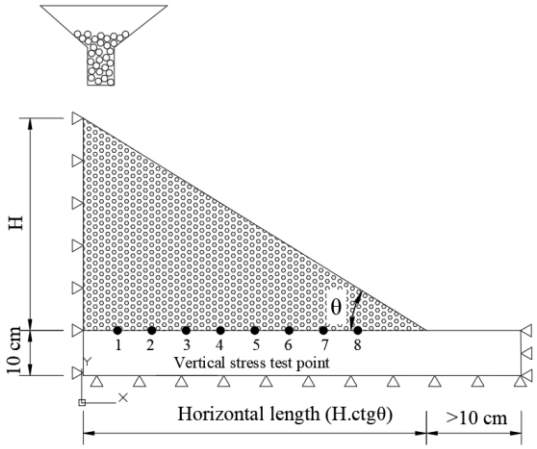

(a) Layout of self-weight stress measurement points of slope

(b) Test box

Fig. 1 – Indoor test scheme

Test conditions

In order to study the influence of various slope heights and slope ratios on the self-weight stress distribution of slope terrain with granular material, multi-condition tests with slope ratios of 1:1.5, 1:2.0, 1:2.5 and 1:3.0 as well as test conditions with slope heights of 30cm, 35cm, 40cm and 45cm are carried on, as shown in Table 1 (a total of 16 test cases).

Tab. 1 - Test conditions

Slope ratios	Slope heights /cm			
	30	35	40	45
1:1.5	√	√	√	√
1:2.0	√	√	√	√
1:2.5	√	√	√	√
1:3.0	√	√	√	√

Test sensor

In terms of pressure test sensors, as shown in Figure 2, a self-made “water bag pressure sensor” is made basing on the communicating vessels principle. Under the action of the upper pressure (the weight of the upper sand), the water in the bag will flow into the pipe, and the pressure is represented by recording the height of the water column. In order to easily observe the change of the water column height, red liquid is dropped into the water bag.

Fig. 2 – Water bag pressure sensor

Test procedure

(1) Level the test box. In order to ensure that the test box is in a horizontal state, level bubbles are placed in the length and width directions of the box bottom side, and the levelling work is completed before starting the test.

(2) Calibration of the water bag pressure sensors. The water bag pressure sensors are preloaded before starting the formal test. Firstly, make sure that the water bag is full, that is, no air bubbles remain. Then pave a 6cm thick quartz sand layer (approximately 2cm above the top surface of the water bag) on the water bags placed side by side, and read the liquid level height before and after paving the sand. On the one hand, it is to confirm whether the liquid level is working normally, on the other hand, it is to compare whether the hydraulic pressure difference of each water bag is consistent, and after the actual calibration, make sure the error is within 0.2mm. The formal test continues to be carried out based on the preload thickness, the test result is based on the difference of the liquid height before and after the formal test.

(3) Formation of quartz sand slope using point source method. The funnel is used to form the slope body by falling sand at the preset slope top position. Since the falling sand is difficult to form different slope ratio cases, the wooden slats are used for slight flattening. For each of the cases shown in Table 1, two sets of parallel tests have been carried out. If there are large deviations on the test results, the third set parallel tests will be supplemented.
(4) Data record. When the slope is formed, in order to reduce the experimental error, keep it stand for 10 minutes, and the reading cannot be carried out until the liquid height is stable. Use a transparent triangular ruler to measure the height of the vertical liquid column, move the liquid column tube slightly to the left and right to record the largest liquid height during the measurement.

ANALYSIS AND DISCUSSION OF THE TEST RESULTS

Vertical stress distribution characteristics of slope terrain

The test results of “slope height 30cm-slope ratio 1:1.5 (case I)”, “slope height 35cm-slope ratio 1:2.0 (case II)”, “slope height 40cm-slope ratio 1:2.5 (case III)” and “slope height 45cm-slope ratio 1:3.0 (case IV)” are extracted and analysed, as shown in Figure 3. The dotted lines in Figure 4 are the corresponding points of the corresponding cases, which are converted to the equivalent height of the water column (referred to the equivalent value of γh) through multiplying the gravity of the quartz sand by the buried depth (γh).

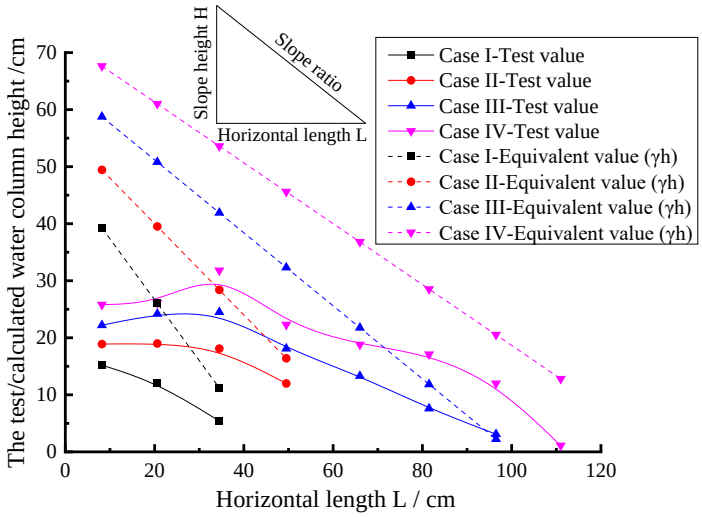

Fig. 3 – Comparison between the test value and the equivalent value γh

It can be seen from Figure 3 that the test value is generally smaller than the equivalent value of γh, and the closer the measuring point is to the top of the slope (namely, the smaller the measuring point number shown in Figure 3), the greater the difference between the test value and the γh equivalent value. At measurement point 1, which is closest to the top of the slope, the actual measured values of cases I ~ IV are only 38.7%, 38.2%, 37.8% and 38.1% of the equivalent value γh of the corresponding cases, respectively. The self-weight stress distribution on the bottom surface of the slope about case I and case II decreases monotonously from the top of the slope to the foot of the slope, that is, the peak stress appears at the measuring point 1; however, the self-weight stress of the slope bottom surface of case III and case IV increases first and then decreases from the top of the slope to the foot of the slope, that is, there is a phenomenon of stress depression, and the peak stress deviates from the actual slope top section to a certain range. In case III, the position where the stress peak appears is about 26.5%L from the top of the slope corresponding to the bottom surface point of the slope, and the peak stress is 58.1%γh of the corresponding point; the position where the stress peak appears in case IV is about 24.1%L from the top of the slope corresponding

to the bottom surface point of the slope, and the peak stress is 53.6% of the γh value of the corresponding point.

Influence of slope height on the distribution of vertical self-weight stress about slope

The experiment photo is shown in Figure 4 (for the condition: slope ratio = 1:1.5 and slope height =40cm) when the slope is formed. Since there are too many experiment conditions involved, in order to better describe in-situ stress distribution of the slope and the convenience of readers, the remaining experiment conditions are represented by curve graphs. The test results of different slope height conditions are extracted with the fixed slope ratio, as shown in Figure 5.

Fig. 4 – The experiment photo after the slope is formed (the condition: slope ratio = 1:1.5 and slope height =40cm)

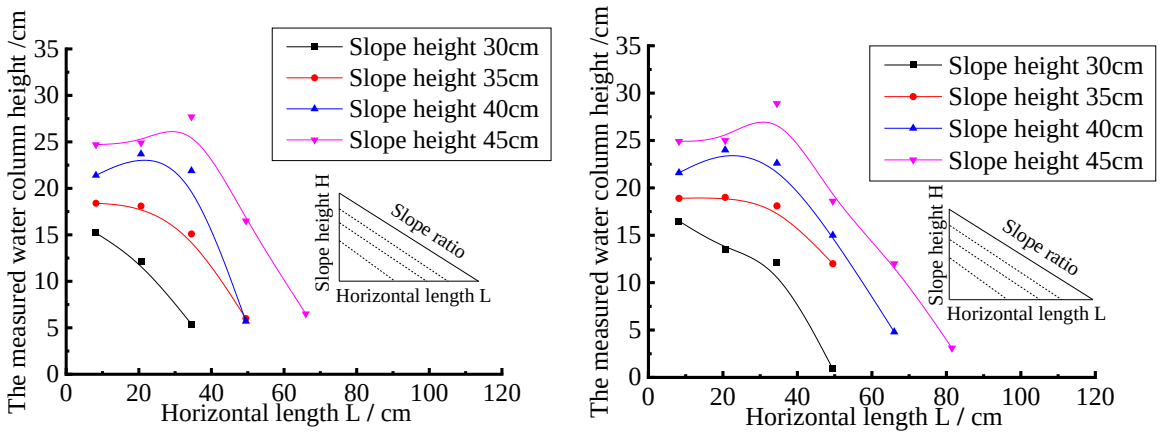

(a) Fixed slope ratio (1:1.5)

(b) Fixed slope ratio (1:2.0)

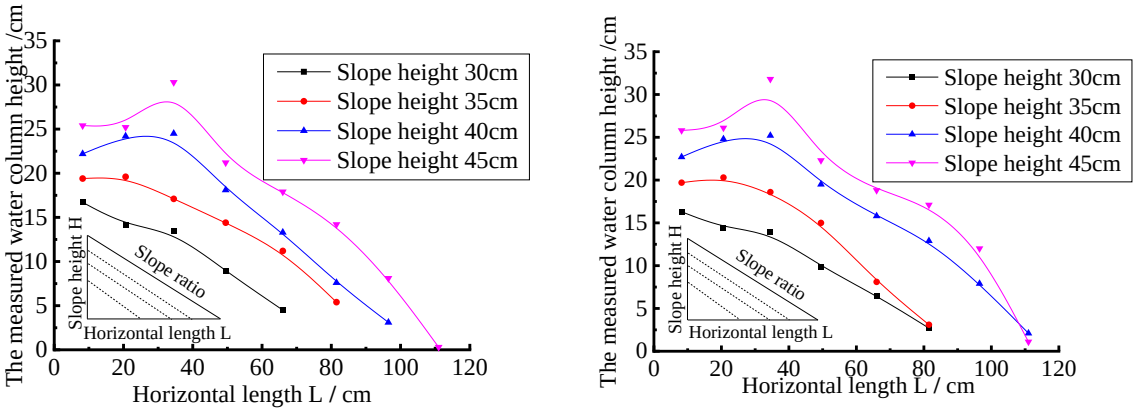

(c) Fixed slope ratio (1:2.5) *(d) Fixed slope ratio (1:3.0)*

Fig. 5 – Influence of slope heights on test results

Figure 5(a) shows that under the condition of the slope ratio 1:1.5, the self-weight stress distribution curve of the slope bottom surface with slope heights of 30cm and 35cm decreases monotonously from the top of the slope to the slope foot, while the curves for the slope heights of 40cm and 45cm appears as a single wave crest that rises first and then falls; the absolute data difference of the adjacent slope heights at measurement point 1 is similar, it is about 3.2cm water column height; the stress peaks of the four slope heights are respectively 31.7%, 32.8%, 35.9%, and 36.2% of the calculated γh value of the corresponding slope height. Figure 5(b) shows under the condition of slope ratio 1:2.0, the self-weight stress distribution curve of the slope bottom surface of the slope height of 30cm decreases monotonously from the top of the slope to the slope foot, while the curve of the slope heights 40cm and 45cm appears to rise first and then fall, showing a single wave crest shape. The data of measuring point 1 and measuring point 2 with the slope height 35cm are almost the same, which can be regarded as the transition state of the above two curve forms. The absolute data difference of the adjacent slope height at measurement point 1 is similar, about 2.8cm water column height. The stress peaks of the four slope heights are respectively 34.4%, 33.9%, 36.6% and 37.4% of the calculated γh value according to the corresponding slope height. Figure 5(c) shows that under the condition of the slope ratio 1:2.5, the self-weight stress distribution curve of the slope bottom surface with a slope height of 30cm decreases monotonously from the top of the slope to the slope foot, while the curves for the slope heights 40cm and 45cm appear to the single wave peak state of rising first and then decreasing, and there is small fluctuations in the slope curve after the peak of the case (slope height 45cm), and the case of slope height 35cm is still the transition state of the above two curve forms; the absolute data difference of the adjacent slope height at measurement point 1 is similar, about 2.9cm water column height; the stress peaks of the four slope heights are 34.8%, 35.0%, 38.0% and 39.0% of the calculated γh value according to the corresponding slope height, respectively. Figure 5(d) shows that under the case of the slope ratio 1:3.0, the self-weight stress distribution curve of the bottom surface of the slope with slope height of 30cm decreases monotonously from the top of the slope to the slope foot, while the curve of the slope heights 40cm and 45cm appears to the single wave peak state of rising first and then falling, and the slope of the post-peak curve of the two slope height cases shows small fluctuations. The data at measuring point 2 of the 35cm slope height case is slightly larger than the data at measuring point 1, and it is about to change from decreasing monotonically to single wave peak state; the absolute data difference of the adjacent slope heights at measuring point 1 is similar, it is about 3.2cm water column height; the stress peaks of the four slope heights are 34.0%, 35.7%, 38.8% and 40.8% of the calculated γh value of the corresponding slope heights.

It can be concluded that when the slope ratio is constant, with the increase of slope height, the self-weight stress distribution curve of the slope bottom surface changes monotonous decrease

from slope top to slope foot to a single peak wave state that first rises and then falls. Under the test conditions, the self-weight stress distribution curve of the slope bottom surface with slope height 30cm under different slope ratios shows a monotonous decreasing shape, while the slope heights of 40cm and 45cm shows a single wave peak shape that first increases and then decreases. The slope height of 35cm is the transitional case of the above two curve forms. The higher the slope height, the more obvious the wave crest, and the farther the wave crest (stress peak) appears from the top of the slope. The stress peak value of all cases is about 31.7%~40.8% of the calculated γh value of the corresponding slope height. If only the single wave peak shape case is considered, the value is 35.9%~40.8%. Affected by the slope heights, the slope of the curve with the same slope ratio does not show a good parallel relationship, but under the same slope ratio, the absolute data difference of the measuring point at the nearest slope top of the adjacent slope height is similar, it is about 2.8~3.2 cm water column height.

Influence of slope ratio on the distribution of vertical self-weight stress about slope

The test results of different slope ratios are extracted with the fixed slope heights, as shown in Figure 6.

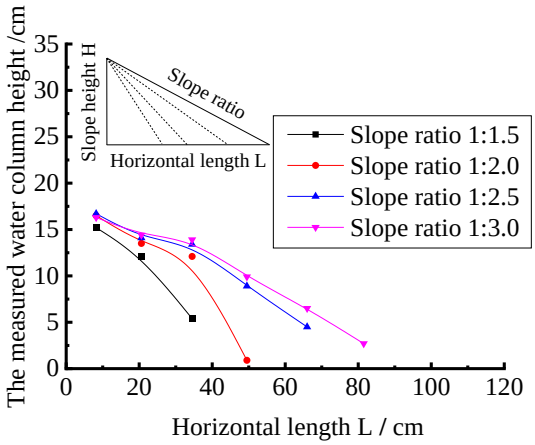

(a) Fixed slope height (30cm)

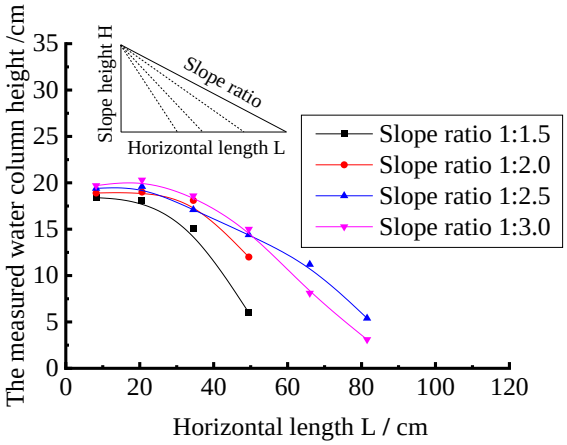

(b) Fixed slope height (35cm)

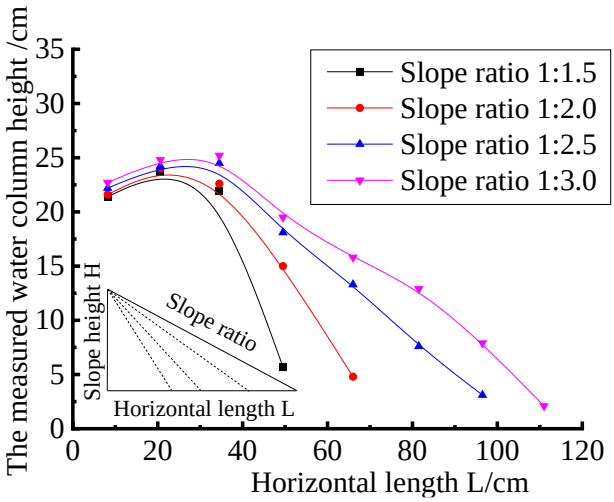

(c) Fixed slope height (40cm)

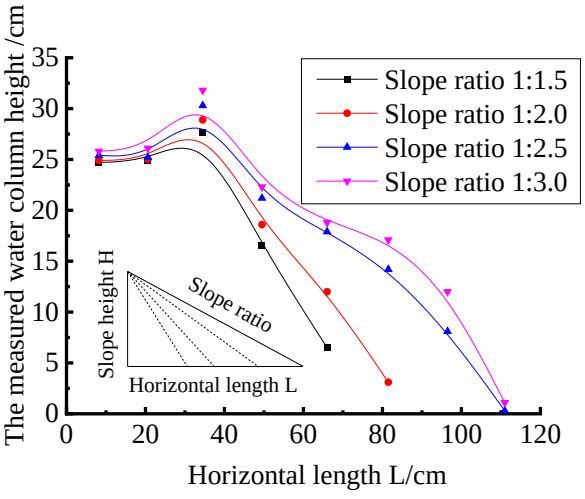

(d) Fixed slope height (45cm)

Figure 6 – Influence of slope ratio on test results

Figure 6(a) shows the measured curves of the four cases with slope ratios of 1:1.5, 1:2.0, 1:2.5 and 1:3.0 under the condition of fixed slope height 30cm. The curves of the above four slope ratios all show a monotonous decrease from the slope top the to the slope foot, and the peak stress point is the measuring point closest to the slope top (measurement point 1), the difference of these four cases is little, and the difference increases with the increase of the distance from the measuring point 1. Figure 6(b) shows the measured curves of the four cases with slope ratios 1:1.5, 1:2.0, 1:2.5 and 1:3.0 under the condition of the fixed slope height 35cm. The shapes of the four curves are similar, and all show that the measured value of measuring point 1 and measuring point 2 are close, that is, the curve of this section is close to horizontal, and then as the number of measuring points increases, the curve shows a downward trend; the curve with slope ratio 1:2.0 crosses the curve with slope ratio 1:2.5, and the curve with slope ratio 1:2.5 crosses the curve with slope ratio 1:3.0, but there is no significant difference in the data of measurement point 1, which is the peak stress. Figure 6(c) shows the measured curves of the 4 cases with slope ratios 1:1.5, 1:2.0, 1:2.5 and 1:3.0 under the condition of the fixed slope height 40cm.The four curves shows the same trend that as the number of the measuring point increases, the curve first increases and then decreases; the peak stress appears between the measuring point 2 and measuring point 3, as the slope ratio decreases (the slope becomes gentler), the more the deviation from the top of the slope is, the less significant is. The tilt rate of the curve after the peak becomes gentle as the slope ratio decreases. Figure 6(d) shows the measured curves of the 4 cases with slope ratios of 1:1.5, 1:2.0, 1:2.5, and 1:3.0 under the condition of a fixed slope height of 45cm. The four curves all appear to increase first and then decrease, presenting a more obvious single wave crest shape, with a stress depression at the top of the slope. In contrast, the curve before the wave crest with the slope height 40 cm is convex, and the curve before the wave crest in this case is concave. The stress peaks all appear between measuring point 2 and measuring point 3, the specific position is not affected by the slope ratio. The distance from the horizontal length 0 point is 29.0cm, 30.8cm, 32.3cm, 32.8cm, respectively; compared with the horizontal length of the corresponding slopes, the ratios are 43.0%, 34.2%, 28.7% and 24.3% respectively. The magnitude of the peak stress increases as the slope ratio decreases. If the maximum value of γh with the slope height 45 cm is used as the reference, the stress peaks of the slope ratios 1:3.0, 1:2.5, 1:2.0 and 1:1.5 are 40.8%, 38.9%, 37.4%, 36.2% of the benchmarks respectively.

It can be concluded that when the slope height remains unchanged, with the decrease of the slope ratio, the shape of the self-weight stress distribution curve at the bottom of the slope shows a good consistency, especially in the section near the slope top, and the data difference of the measurement point 1 closest to the top of the slope is minimal. For cases of the slope heights 40cm and 45cm where the distribution curve is in the form of a single wave peak, the smaller the slope ratio, the more obvious the wave crest, and the farther away the wave crest appears from the slope top, but it is not significant. For the curve section before the wave crest, the 40cm slope height case is convex, while the 45cm slope height case is concave. For the slope of the post-peak curve with the same slope height, the change law is roughly the same as the slope ratio. The smaller the slope ratio, the smoother the curve.

CONCLUSION

Based on the quartz sand slope formed by the point source method with granular material, the experimental research on the vertical self-weight stress distribution of the slope terrain under different conditions is carried out. The main conclusions are as follows.

(1) The test value is generally smaller than the γh equivalent value, and the closer the measuring point is to the slope top, the greater the difference between the test value and the γh equivalent value. At measurement point 1, which is closest to the slope top, the measured values are only 38.7% of the calculated equivalent value of γh in the corresponding cases. The vertical self-weight

stress distribution of granular material slope terrain may show the phenomenon of slope crest stress depression after the slope reaches a certain height, and the range of the stress depression is mainly related to the slope height, while the slope ratio has little effect on this.

(2) With the fixed slope ratio, as the slope height increases, the self-weight stress distribution curve on the bottom of the slope changes from a monotonous decrease to the state that: from the slope top to the slope foot being with a single wave crest that rises first and then drops, and the higher the slope height, the more obvious the wave crest, and the farther the wave crest (stress peak) appears from the slope top.

(3) With the fixed slope height, the shape and trend of the self-weight stress distribution curve of the bottom surface of the slope with different slope ratios are similar. When the slope height reaches a certain value, the crest of the self-weight stress distribution curve at the bottom of the slope is more prominent, and the farther the position of the wave crest deviates from the slope top section, but it is not significant.

ACKNOWLEDGMENTS

The authors would like to acknowledge the financial support of the National Natural Science Foundation of China (51578459).

REFERENCES

[1] Guan, B. S., 2003. Key Points of tunnel engineering design. China Communication Publishing, Beijing.

[2] Zhang, N., 2002. Study on the current crustal stress field in the rockmass. Master's thesis, Zhejiang University, Hangzhou.

[3] Xie, K. H., Hu, A. F., Liu, Y. M., 2004. On computation of overburden pressure and settlement for layered soil considering sedimentation. Chinese Journal of Rock Mechanics and Engineering, Vol. 23, 1585-1589.

[4] Liu, Y. and Li, W., 2001. Gravitational stresses in parallel stratified rock mass. Rock and Soil Mechanics, Vol. 22: 63-66. https://doi.org/10.16285/j.rsm.2001.01.017

[5] Liang, Y., 2008. The study of in situ stress and rock slope stability analysis in deep-incised valley. Ph.D thesis, Southwest Jiaotong University, Chengdu.

[6] Savage, W. Z., 1993. Gravity-induced stresses near a vertical cliff. International Journal of Rock Mechanics and Mining Science & Geomechanics Abstracts, Vol. 30: 325-330. https://doi.org/10.1016/0148-9062(93)91716-V

[7] Savage, W. Z., 1994. Gravity-induced stresses in finite slopes. International Journal of Rock Mechanics and Mining Sciences & Geomechanics Abstracts, Vol. 31: 471- 483. https://doi.org/10.1016/0148-9062(94)90150-3

[8] Yu, D. J., Zhu, W. S., Yong, M., et al., 2011. Initial geostress field characters in mountain with different slopes and its influence on underground projects. Rock and Soil Mechanics, Vol. 32: 609-613. https://doi.org/10.16285/j.rsm.2011.s1.060

[9] Qi, S. W. and Wu, F. Q., 2011. Stresses field characteristics of a valley slope in high geo-stress area. Rock and Soil Mechanics, Vol. 32: 1460-1464. https://doi.org/10.16285/j.rsm.2011.05.019

[10] Zhao, D. A., Chen, Z. M., Cai, X. L., et al., 2007. Analysis of distribution rule of geostress in China. Chinese Journal of rock mechanics and Engineering, 1265-1271.

[11] Savage, W. Z., Swolfs, H. S., Powers, P. S., 1985. Gravitational stresses in long symmetric ridges and valleys. International Journal of Rock Mechanics and Mining Sciences & Geomechanics Abstracts, Vol. 22: 291- 302. https://doi.org/10.1016/0148-9062(85)92061-3

[12] Mctigue, D. F. and Mei, C. C., 1981. Gravity-induced stresses near topography of small slope. Journal of Geophysical Research Solid Earth, Vol. 86: 9268-9278. https://doi.org/10.1029/JB086iB10p09268

[13] Mctigue, D. F. and Mei, C. C., 1987. Gravity-induced stresses near axisymmetric topography of small slope. International Journal for Numerical and Analytical Methods in Geomechanics, Vol. 11: 257-268.

[14] Mandal, P. and Singh, R. N., 1991. Gravity induced near-surface stresses in long-symmetric ridge-valley systems. Journal of Earth System Science, Vol. 100: 267-280.

[15] Wang, H. Y., Chen, S. M., Yan, Z. X., 2008. Principles of dynamic design of underground engineering. Chemical Industry Press, Beijing.
[16] Vernay, M., Morvan, M., Breul, P., 2020. Experimental study on the influence of saturation degree on unstable behavior within granular material. European Journal of Environmental and Civil Engineering, Vol. 24: 1821-1839. https://doi.org/10.1080/19648189.2018.1488623
[17] Wu, Q. X., Yan, L. Y., Yang, Z. X., 2021. Discrete element simulations of drained granular material response under multidirectional rotational shear. Computers and Geotechnics, Vol. 139: 104375(1-13) https://doi.org/10.1016/j.compgeo.2021.104375
[18] Chen, W. B., Feng, W. Q., Yin, J. H., 2020. Effects of water content on resilient modulus of a granular material with high fines content. Construction and Building Materials, Vol. 236: 117542(1-14). https://doi.org/10.1016/j.conbuildmat.2019.117542
[19] Chen, X. X., 2018. The research of stability of rock slope based on statistics and particle flow code. Master's thesis, Jilin University, Jilin.
[20] Tang, H. M., Yan, Z. Q., Chen, H. K., 2016. Numercial simulation on failure of Gongjiafang 2# bank slope in Wu Gorge of the three gorges based on discrete element method. Journal of Choingqin Normal University (Natural Science), 33(1): 40-46. https://doi.org/10.11721/cqnuj20160128
[21] Hou, J., Zhang, M. X., Chen, Q., et al, 2019. Failure-mode analysis of loose deposit slope in Ya'an-Kangding Expressway under seismic loading using particle flow code. Granular Matter, 21(1), 1-12. https://doi.org/10.1007/s10035-018-0859-1
[22] Li, X. X, Liu, J. S, Gong, W. P., et al, 2022. A discrete fracture network based modeling scheme for analyzing the stability of highly fractured rock slope. Computers and Geotechnics, 141, 104558(1-18). https://doi.org/10.1016/j.compgeo.2021.104558
[23] Bu, X. H., Fu, R. H., Li, J. D., et al, 2016. Internal Factors of the Failure of Granular Mixtures Slope, Journal of Yangtze River Scientific Research Institute, 33(9): 116-120. https://doi.org/10.11988/ckyyb.20150606
[24] Zhang, J. M., Luo, Y., Zhou, Z., et al, 2021. Effects of preferential flow induced by desiccation cracks on slope stability. Engineering Geology, 288, 106164(1-16). https://doi.org/10.1016/j.enggeo.2021.106164
[25] Sun, Q. C. and Wang, G. Q., 2009. Introduction to particle mechanics. Science Press, Beijing.
[26] Luo, W. Z., 2020. Experimental study and analysis on stress arch effect in sand. Master's thesis, South China University of Technology, Guangzhou.
[27] Yao, Y. X., Li, S., He, C., et al, 2019. Analysis on pressure characteristic at bottom of sand heap with laboratory experiment and PFC2D numerical simulation. Journal of Engineering Geology, Vol. 27: 1281-1289.